

Plankton Food Web and its Seasonal Dynamics in a Large Monsoonal Estuary (Cochin backwaters, India) - Significance of Mesohaline Region

¹P.M. Sooria, *¹R. Jyothibabu, ¹A. Anjusha, ¹G. Vineetha, ¹J. Vinita, ¹K. R. Lallu, ¹M. Paul, ¹L. Jagadeesan

¹CSIR –National Institute of Oceanography, Regional Centre, Kochi, India

*Corresponding author, Email - rjyothibabu@nio.org, Phone - 91 (0) 484 2390814, Fax - 91 (0) 484 2390618

Abstract

The paper presents the ecology and dynamics of plankton food web in the Cochin backwaters (CBW), the largest monsoonal estuary along the west coast of India. The data source is a time series measurement carried out in the CBW during the Spring Intermonsoon (March - May) and the Southwest Monsoon (June - September). The plankton food web consisting of autotrophic/heterotrophic picoplankton, autotrophic/heterotrophic nanoplankton, micro-zooplankton and meso-zooplankton was quantified in relation to the seasonal hydrographical settings in the CBW. The study showed that significant changes in the abundance and dynamics of plankton food web components were governed mostly by the spatial and seasonal changes in hydrography rather than short-term changes induced by tide. During the Spring Intermonsoon, all plankton consumers in the CBW was higher than the Southwest Monsoon, and the trophic interaction was more effective in upstream where there was a close coupling between all prey components and their consumers. During the Southwest Monsoon, on the other hand, the trophic interaction was more effective downstream where the abundance of all plankton consumers was significantly higher than the upstream. Based on statistical analyses SIMPROF/NMDS and RDA, we demarcated the spatial difference/mismatch in the prey and consumer distribution in the CBW and showed that a more efficient plankton food web exists in the mesohaline regions during both seasons. This suggests that a noticeable spatial shift occurs seasonally in the active plankton food web zone in the CBW; it is upstream during the Spring Inter monsoon and downstream during the Southwest Monsoon.

Key words - Plankton. Copepods. Multivariate Analyses. Cochin backwaters. Arabian Sea

1. Introduction

Estuary, the transition zone of river and sea, mediates carbon flux between terrestrial and marine ecosystems. They are dynamic primarily due to short-term changes caused by tide and the seasonal changes induced by the regional climate (Madhupratap and Rao 1979; Iriarte and Purdie 1994). Tide causes changes in salinity and nutrients distribution, which potentially impact the spatial distribution of biological components (Iriarte and Purdie 1994; Madhupratap 1987; Kimmerer et al. 1998). On the other hand, due to seasonal changes, an estuary can exhibit significant variations in the distribution of physicochemical as well as biological components (Madhupratap 1987; Jyothibabu et al. 2006).

India has about 25 estuaries located along its 7500 km coastline (Qasim 2003) of which those heavily influenced by the Southwest Monsoon (June – September) rainfall are referred to as Monsoonal Estuaries (Vijith et al. 2009). Based on a comprehensive data set, we introduce in this paper the dynamics and distribution ecology of plankton food web components in the largest monsoonal estuary along the west coast of India. This study is germane to the fact that an efficient feeding interaction in a plankton food web takes place when two primary conditions are satisfied (a) high efficiency of the consumer to feed on the available prey and (b) co-existence of adequate population of consumer and prey in space and time (Azam et al. 1983; Landry and Fagerness 1988; Landry et al. 2008; Garrison et al. 2000; Calbet and Landry 2004).

Improved understanding of the spatial and seasonal hydrographical settings and its impacts on biological components in monsoonal estuaries in the last decade guided us to conceptualize a possible spatial mismatch in the distribution of various plankton components in the food web (Menon et al. 2000; Ram et al. 2003; Jyothibabu et al. 2006; Madhu et al. 2007; Thottathil et al. 2008 a & b). In order to evaluate the hypothesis, we quantified the plankton food web in a monsoonal estuary during the Spring Intermonsoon (dry season) and Southwest Monsoon (wet season). The objectives of the present study can be outlined as (a) to characterize the dynamics and distribution ecology of different functional components of plankton food web and (b) to understand the spatial and temporal changes in plankton food web components to suggest the trophic pathways existing in different environmental settings in a monsoonal estuary.

The literature on the hydrobiology of CBW consists of isolated studies on heterotrophic bacteria, phytoplankton, microzooplankton and mesozooplankton (Madhupratap 1987; Jyothibabu et al. 2006; Madhu et al. 2007; Thottathil et al. 2008a). Integrated information on various functional components

of the plankton food web is absent from Monsoonal estuaries. Keeping this in mind, we present in this paper a comprehensive seasonal time-series data of plankton food web from the CBW.

2. Materials and Methods

2.1. Study Area

In monsoonal estuaries, heavy rainfall and river influx during the Southwest Monsoon cause drastic changes in hydrography as the total fresh water inflow becomes several orders of magnitude larger than the estuarine volume (Vijith et al. 2009). The largest monsoonal estuary along the west coast of India is the Cochin Backwaters (CBW), which receives freshwater inflow from seven rivers and salinity incursion from the neighboring Arabian Sea (Fig. 1). The CBW is a complex shallow estuary (average depth 4m), located parallel to the coastline of India between 9° 30' - 10° 10' N and 76° 15' - 76° 25' E (Fig. 1). It extends around 75 km along the coastline and has two permanent inlets to the Arabian Sea - the southern inlet located at Kochi and the northern at Azhikode. As the rivers bring enormous freshwater during the peak Southwest Monsoon (July – August), the CBW transforms into a freshwater lake except near the inlet region (Madhupratap 1987; Qasim 2003; Jyothibabu et al. 2006). Conversely, during the Spring Intermonsoon/Pre-Monsoon (March - May), low freshwater inflow of rivers allows active salinity incursion and, as a result, the downstream of the CBW transforms into an extension of the adjacent Arabian Sea (Madhupratap 1987; Qasim 2003, Jyothibabu et al. 2006).

2.2. Sampling and Methods

Three hourly time series sampling was conducted in four locations in the CBW during the Spring Intermonsoon (March, 2009) and the Southwest Monsoon (September 2009). The seasons were classified based on the internationally accepted JGOFS protocol (UNESCO, 1994). Out of four sampling locations along the salinity gradients in the CBW (L1 to L4), two locations each represented the downstream (L1 and L2) and the upstream (L3 and L4) regions (Fig. 1). During the seasonal sampling, field measurements began at 09.00 hours and ended at 09.00 hours the next day (24 hours). Water samples for various environmental and biological parameters were collected from the surface waters (0.5m) using a Niskin sampler.

2.3. Physicochemical Parameters

Tide in all the four time series locations was measured using tide gauges and readings were taken at every 10 minutes. Surface salinity was measured using a digital salinometer (Make TSK). Dissolved oxygen was estimated by the Winkler's method. Dissolved inorganic nutrients nitrate

(NO₃), phosphate (PO₄) and silicate (SiO₄) were measured following standard colorimetric techniques (Grasshoff et al., 1983). Chlorophyll *a* (hereafter chlorophyll) was measured by filtering 500ml water samples through GF/F filters. The chlorophyll content in phytoplankton cells concentrated on the filter papers was extracted in 10 ml 90% acetone and measured using a Turner fluorometer (UNESCO 1994).

2.4. Picoplankton

Water samples (10 ml) preserved in glutaraldehyde were processed for estimating picoplankton. Samples prefiltered through 3µm sterile glass filters, to remove larger particles, were used to quantify autotrophic and heterotrophic picoplankton (Porter and Feig, 1980). The heterotrophic picoplankton (=heterotrophic bacteria) sample was stained with DAPI, whereas, autotrophic picoplankton samples were processed without any staining. The samples (2 ml) for autotrophic and heterotrophic picoplankton were separately passed through 0.2 µm black nucleopore filters and mounted in immersion oil. The slides were examined under an Olympus BX 53 epifluorescence microscope equipped with an image analyzer (progRes Capture Pro 2.6) under UV excitation for DAPI and blue excitation for phototrophic components. The microscopic analysis was carried out as soon as the slide was prepared, and, in any case, not later than a few hours of its preparation (Bloem et al., 1986). This approach ensured the preservation of autofluorescence of photosynthetic pigments in the samples. The carbon biomass of autotrophic and heterotrophic picoplankton was estimated based on the conversion factors presented in Garrison et al., (2000).

2.5. Nanoplankton

Water samples (15 ml) preserved in glutaraldehyde were very gently pre-screened through 20 µm bolting silk to discard particles >20 µm size. The filtrate was stained with 1.65 µg ml⁻¹ proflavin hemisulfate and filtered through 0.8µm pore sized Nucleopore filter (Haas 1982). This filter is mounted in immersion oil and analyzed under Epifluorescence microscope not later than a few hours of its preparation (Bloem et al. 1986). All organisms between 2 to 20 µm body sizes that fluoresced green under blue illumination were considered as heterotrophic nanoplankton (= heterotrophic nanoflagellates). The phototrophs were separated from the heterotrophs by the presence of red or red-orange autofluorescence of photosynthetic pigments. The counts of heterotrophic and autotrophic nanoplankton were taken using the image analyzer. The carbon biomass of these components were measured based on their body dimensions using the image analyzer and their biovolume calculated by assuming appropriate geometrical shapes (Garrison et al. 2000). The mean biovolume was extrapolated to the total counts at each location to obtain the total biovolume of the nanoplankton

fraction. The conversion of biovolume to organic carbon was carried out based on the numerical conversion factors of Garrison et al. (2000).

2.6. Micro - and Meso – zooplankton

Water samples (1L) for microzooplankton were gently pre-filtered through a 200 μm bolting silk, preserved in acid Lugol's and stored in black polythene bottles. After 48 hours of gravity settling, the water sample was concentrated to ~ 100 ml and again allowed to settle under gravity in a settling chamber for 48 hours. The settled samples were observed under an inverted microscope with an image analyzer (Olympus IX 51). The microzooplankton community was broadly grouped into ciliates, heterotrophic dinoflagellates and crustacean larvae. Ciliates and heterotrophic dinoflagellates were identified up to the species level based on available literature (Kofoid and Campbell 1939; Subrahmanian 1971; Maeda 1986; Krishnamurthy et al. 1995).

The mesozooplankton was collected using a WP net (mesh size 200 μm , mouth area 0.28 m^2). The net was towed horizontally just below the water surface for 10 minutes. A digital flow meter (Hydro Bios, Model- 438110) was attached across the net opening to estimate the amount of water filtered to collect the sample. The zooplankton biomass was measured following the standard displacement volume method after removing large detrital particles (Harris et al. 2000). The displacement volume of zooplankton was converted into dry weight using a factor of 0.075 g. dry wt. ml^{-1} and then to carbon biomass following the standard conversion factor of Madhupratap et al. (1981).

2.7. Analysis of Variance (ANOVA)

Standard statistical treatments were used to analyze the significance of tidal as well as seasonal variation on various hydrographical and biological parameters. First, the environmental and biological data were tested for their normal distribution and homogeneity. For data with the normal distribution, parametric ANOVA with Tukeys HSD post hoc test was used to compare the significance. In the case of data with clumped distribution, non-parametric ANOVA (Kruskal-wallis) with Dunn's post hoc test analyzed the significance of differences. The tests of normality, parametric and nonparametric ANOVA were carried out in XL stat pro-software package.

2.8. Cluster / SIMPROF and NMDS

Cluster/ SIMPROF and NMDS were used to segregate the observations of different parameters into clusters based on their similarity/homogeneity. The data or observation in one cluster indicates their similarity or homogeneity whereas their placement in different clusters shows the dissimilarity or heterogeneity. The data of plankton food web components were initially standardized and log

(X+1) transformed to normalize the differences in numerical abundance (Clarke and Warwick 1994). The Bray-curtis similarity matrix based on group average method was used to understand the spatial grouping of observations during different seasons.

2.9. Dominant Species Index

The Dominant Species Index is used to find out the most common and numerically abundant species in each group of observations or locations. Dominant species of ciliates and heterotrophic dinoflagellates in each location during the Spring Intermonsoon and Southwest Monsoon were calculated using the standard equation (Yang et al. 1999; Lee et al. 2009; Lin et al. 2011).

$$Y_i = (N_i/N) \times f_i$$

Where, Y_i is the dominance of species i , N_i is the number of individuals of species i in all locations, N is the number of individuals of all species in all locations, and f_i is the frequency of locations at which species i occurs. The species with Y_i value ≥ 0.02 were considered as dominant species.

2.10. Redundancy Analysis (RDA)

The interrelationships between the plankton components and their environmental variables were analyzed by RDA models (CANOCO 4.5). Initially, the data was analyzed using Detrended Correspondence Analysis (DCA) to select the appropriate ordination technique. The result of DCA showed axis gradient length < 2 suggesting that linear multivariate RDA was suitable for the present case (Birks 1998; Leps and Smilauer 2003) with species correlation scaling as ordination scores. The biological variables were log transformed prior to the analysis. Partial RDA was also carried out to find out the environmental parameters contributing more to the explained variation in the biological components. The ordination significance was tested with Monte Carlo permutation tests (499 unrestricted permutations) ($p < 0.05$). The results of the RDA are presented in the form of Triplots in which the time series samples are displayed by points and environmental variables by arrows. Arrows for species abundance and environmental variables indicate the direction in which the corresponding parameters increase (Leps and Smilauer 2003).

3. Results

3.1. Hydrography

3.2. Spring Intermonsoon

The changes in tidal phase and salinity distribution in the CBW (L1 - L4) during the Spring Intermonsoon have been presented in Fig. 2. The average tidal height in the inlet region was 0.7m,

which decreased towards the upstream (0.5m). The tidal rhythm was distinct in salinity distribution, more prominently downstream; euhaline waters dominated in the downstream sites and mesohaline waters upstream (Fig. 2a). The highest and lowest salinity values were recorded at L1 downstream (av. 29.15 ± 2.78) and L4 upstream (av. 9.94 ± 0.02), respectively (Table 1). In all locations, the highest/lowest salinity coincided with the highest/lowest tidal amplitude. The tidal phase in the upstream sites showed a time lag from that in the downstream sites, and so was the salt intrusion. Salinity showed minor tidal variation in all the sampling locations, but significant spatial variation was observed between the upstream and the downstream (Supplementary ANOVA Table 1). The dissolved oxygen concentration was generally high in the entire study area with higher values in the mesohaline upstream region as compared to the downstream. The dissolved oxygen was the highest at L4 in the upstream region (av. $5.96 \pm 0.15 \text{ mg L}^{-1}$) and the lowest at L1 downstream (av. $3.87 \pm 0.18 \text{ mg L}^{-1}$). The tidal variation of dissolved oxygen was minor in all the study locations (Table 1).

Nitrate (NO_3) concentration was remarkably high in the entire study area and showed minor tidal variations except in L1, in the downstream region (Table 1). The distribution of phosphate (PO_4) showed an increasing trend towards the downstream whereas the trend exhibited by silicate (SiO_4) concentration was vice versa (Table 1). While the tidal variation in PO_4 was significant only in the downstream locations, SiO_4 variation was significant at L2 and L3 (Table 1). The spatial difference in PO_4 and SiO_4 was significant between the upstream and the downstream (Supplementary ANOVA Table 1). The chlorophyll concentration throughout the study area was generally high with the highest at L3 (av. $18.46 \pm 0.99 \text{ mg m}^{-3}$) and the lowest at L1 (av. $3.99 \pm 0.45 \text{ mg m}^{-3}$). The tidal variation of chlorophyll was significant only in L2 and L3, but their spatial variation was significant between L1 downstream and all other locations (L2, L3 and L4) (Supplementary ANOVA Table 1). Overall trend in the distribution of physicochemical parameters showed significant spatial variations between the downstream and the upstream (Supplementary ANOVA Table 1).

3.3. Southwest Monsoon

The CBW was heavily influenced by fresh water, which caused low tidal amplitude in the upstream region (Fig. 3). The tidal height was noticeably low in the downstream regions (0.5m), which decreased further towards the upstream (0.2m). The large freshwater influx led to a drastic drop in salinity and an increase in the duration of low tide. The average surface salinity was significantly low in the entire stretch of the study area (0.10 to 8.66). Relatively high saline/mesohaline conditions (av. 8.62 - 8.66) were found downstream while extremely low saline

conditions (av. 0.1 – 2.11) were encountered upstream (Table 1). Due to high advection of freshwater from the upstream, the phase lag in tidal propagation and salinity intrusion in the upstream area was very weak (Fig. 3). Even though the tidal variation in salinity was between oligohaline to mesohaline ranges, these variations were large in all the locations except the L4 site upstream (Table 1). Similarly, the spatial variation in salinity was significant between all the locations except L1 and L2 in the downstream and L3 and L4 in the upstream area (Supplementary ANOVA Table 1). The dissolved oxygen concentration was generally high in the entire study area with the highest at L4 and the lowest downstream (Table 1). The tidal variation of dissolved oxygen during the study period was infinitesimal in all the study locations (Table 1).

The nitrate (NO_3) concentration was generally high in the study area (Table 1). The spatial distribution of NO_3 did not show any noticeable pattern and the highest and lowest values were found in L1 and L3, respectively (Table 1). The tidal fluctuation of NO_3 was small in all locations (Table 1) whereas, spatial variation in its distribution was significant (Supplementary ANOVA Table 2). The distribution of phosphate (PO_4) and silicate (SiO_4) also showed a clear spatial trend; the former increased downstream and the latter upstream (Fig. 3). The tidal variation of PO_4 and SiO_4 in the study area was small in all locations (Table 1). The chlorophyll was generally high throughout the study area with significant tidal variations in the downstream region (Table 1). The overall trend in distribution of all physicochemical parameters except the salinity showed low tidal variations. On the other hand, there was a more prominent spatial variation in hydrographical parameters between the downstream and the upstream (Supplementary ANOVA Table 1).

3.4. Plankton Food Web

A schematic picture of a typical plankton food web in an estuarine system is presented in Fig. 4a. The subsequent panel presents the photomicrographs of the plankton components quantified during the present study (Fig. 4b-g). The distribution of various plankton components in relation to the salinity ingress and egress associated with tidal action during the Spring Intermonsoon and the Southwest Monsoon has also been presented in Fig. 5 and 6. Detailed information on the abundance and distribution of each plankton component in the temporal and spatial environmental settings in the study area is presented in the following sections.

3.5. Picoplankton

The tidal and spatial variation of autotrophic and heterotrophic picoplankton during the Spring Intermonsoon is presented in Table 1. Similarly, the abundance of autotrophic and heterotrophic picoplankton in relation to changes in salinity during the Spring Intermonsoon is presented in Fig. 5a

&b. The abundance of autotrophic picoplankton was higher upstream as compared to the downstream. The autotrophic picoplankton abundance and biomass were the highest at L4 (av. 3.46×10^7 No. L^{-1} and av. 8.65 mgC m^{-3}) and the lowest at L1 (av. 1.80×10^7 No. L^{-1} and av. 4.5 mgC m^{-3}). In all study locations, autotrophic picoplankton showed only low tidal variation (Table 1) whereas their spatial variation was significant between the downstream and the upstream locations (Supplementary ANOVA Table 1). The abundance and biomass of heterotrophic picoplankton showed relatively high values in the downstream sites (Table 1). The heterotrophic picoplankton abundance and biomass were the highest at L1 (av. 2.20×10^9 No. L^{-1} and av. 24.2 mgC m^{-3}) and the lowest at L4 (av. 1.53×10^9 No. L^{-1} and av. 16.8 mgC m^{-3}). The tidal variation in the abundance of heterotrophic picoplankton was significant only in the downstream locations (Table 1). The spatial variation of heterotrophic picoplankton was significant between the downstream and the upstream sampling sites (Supplementary ANOVA Table 1).

During the Southwest Monsoon, the abundance and biomass of autotrophic picoplankton were higher downstream as compared to the upstream (Table 1). The abundance of autotrophic and heterotrophic picoplankton in relation to changes in salinity during the Southwest Monsoon has been presented in Fig. 6a & b. The abundance and biomass of autotrophic picoplankton were the highest at L2 (av. 1.52×10^7 No. L^{-1} and av. 0.25 mgC m^{-3}) and the lowest at L4 (av. 0.07×10^8 No. L^{-1} and av. 0.2 mgC m^{-3}). The heterotrophic picoplankton abundance and biomass during the Southwest Monsoon was noticeably higher downstream as compared to upstream. The highest heterotrophic picoplankton abundance and biomass were found at L2 (av. 1.26×10^9 No. L^{-1} and av. 13.9 mgC m^{-3}) and the lowest at L4 (av. 0.80×10^9 No. L^{-1} and av. 7.92 mgC m^{-3}). The tidal variation in autotrophic and heterotrophic picoplankton was found to be minor in all locations during the Southwest Monsoon whereas their spatial variation was significant between the upstream and the downstream locations (Table 1, Supplementary ANOVA Table 1). The abundance of heterotrophic picoplankton showed marked seasonal variations in all the study locations whereas autotrophic picoplankton showed significant seasonal variation only in the upstream locations (Supplementary ANOVA Table 2).

3.6. Nanoplankton

During the Spring Intermonsoon, the abundance and biomass of autotrophic nanoplankton showed an increasing trend towards the upstream (Table 1). The abundance of autotrophic and heterotrophic nanoplankton in relation to the changes in salinity during the Spring Intermonsoon is presented in Fig. 5c. The autotrophic nanoplankton abundance and biomass were the highest in L3

(av. $3.02 \times 10^7 \text{ L}^{-1}$ and av. 645.7 mgC m^{-3}) while the lowest was observed in L1 (av. $0.76 \times 10^7 \text{ L}^{-1}$, av. 162.5 mgC m^{-3}). During the period, the tidal variation of autotrophic nanoplankton was found significant at L2 and L3 (Table 1). The abundance and biomass of heterotrophic nanoplankton were significantly higher in the mesohaline upstream as compared to the downstream sites (Fig. 5d). The heterotrophic nanoplankton abundance and biomass were the highest in L3 (av. $2.6 \times 10^6 \text{ L}^{-1}$ and av. 16.4 mgC m^{-3}) and the lowest in L2 (av. $1.26 \times 10^6 \text{ L}^{-1}$ and av. 7.8 mgC m^{-3}) (Table 1). The heterotrophic nanoplankton distribution showed significant spatial dissimilarity between the upstream and downstream sites (Supplementary ANOVA Table 1).

During the Southwest Monsoon the autotrophic nanoplankton did not show any clear-cut spatial trend between the upstream and downstream locations (Fig. 6c). Their abundance and biomass were the highest in L2 (av. $1.69 \times 10^7 \text{ L}^{-1}$ and av. 324.9 mgC m^{-3}) while the lowest abundance and biomass (av. $0.73 \times 10^7 \text{ L}^{-1}$ and av. 156.1 mgC m^{-3}) were observed in L1. During the study period, autotrophic nanoplankton showed low tidal variation in all locations (Table 1), but their spatial variation was significant between L1 and the upstream sites (Supplementary ANOVA Table 1). The spatial difference in heterotrophic nanoplankton during the Southwest Monsoon showed noticeably higher values downstream as compared to upstream (Fig. 6d). The heterotrophic nanoplankton abundance and biomass was the highest in L2 (av. $1.25 \times 10^6 \text{ L}^{-1}$ and av. 7.1 mgC m^{-3}) and the lowest in L3 (av. $0.43 \times 10^6 \text{ L}^{-1}$ and av. 2.7 mgC m^{-3}). The heterotrophic nanoplankton distribution showed significant spatial difference between the upstream and downstream regions whereas their tidal variation was significant only upstream (Table 1). The abundance of autotrophic and heterotrophic nanoplankton showed prominent seasonal variations upstream, but only minor variations downstream (Supplementary ANOVA Table 2).

3.7. Microzooplankton

The microzooplankton community was composed of ciliates, heterotrophic dinoflagellates and copepod nauplii. The species composition of microzooplankton and their dominance in the community are presented in Table 2. Loricated ciliates belonging to Genus *Tintinnopsis* was predominant during both seasons. During the Spring Intermonsoon, microzooplankton abundance and biomass was noticeably higher upstream than downstream (Fig. 5e). The highest and lowest abundance and biomass were recorded in L3 (av. $3.11 \times 10^4 \text{ No. L}^{-1}$ and av. 340 mgC m^{-3} respectively) and L1, respectively (av. $1.11 \times 10^4 \text{ No. L}^{-1}$ and av. 121 mgC m^{-3} respectively). The tidal variation in microzooplankton abundance and biomass was minor in all locations (Table 1) whereas their spatial variation was significant between the upstream and the downstream locations

(Supplementary ANOVA Table 1). During the Southwest Monsoon, the abundance and biomass of microzooplankton community was noticeably low in upstream than downstream. The microzooplankton showed highest abundance and biomass at L1 (av. 1.98×10^4 No. L^{-1} and av. 216 mgC m^{-3}) while the lowest was observed at L4 (av. 0.48×10^4 No. L^{-1} and av. 52.50 mgC m^{-3}). The tidal variation in microzooplankton abundance was minor in the entire study area (Table 1) whereas the spatial variation was significant between the upstream and downstream sites (Supplementary ANOVA Table 1). The seasonal variation in abundance of microzooplankton was large in the upstream location but insignificant downstream (Supplementary ANOVA Table 2).

3.8. Mesozooplankton

High zooplankton biomass was found throughout the study area during the Spring Intermonsoon with an increasing trend towards the upstream (Table 1; Fig. 5f). The highest zooplankton biomass was recorded at L4 (av. $11.7 \pm 1.3 \text{ mgC m}^{-3}$), followed by L3 (av. $8.02 \pm 0.96 \text{ mgC m}^{-3}$) in the upstream region. The zooplankton biomass over 24 hour time series sampling showed significant tidal variations in all the locations (Table 1). On the other hand, the spatial variation in zooplankton biomass distribution was significant only between the upstream and the downstream sites (Supplementary ANOVA Table 1). During the Southwest Monsoon, the zooplankton biomass is significantly lower than that during the Spring Intermonsoon. Relatively high zooplankton biomass was found in the downstream region during the Southwest Monsoon as compared to upstream (Fig. 6f); the highest was observed in L1 (av. $0.48 \pm 0.5 \text{ mgC m}^{-3}$) and the lowest in L3 (av. $0.24 \pm 0.96 \text{ mgC m}^{-3}$) (Table 1). The variation in mesozooplankton biomass over 24 hour time series sampling showed large variations in the upstream sites while it was small in the case of downstream locations (Table 1). The spatial variation in mesozooplankton biomass was found to be significant only between L1 and the upstream locations (L3 and L4) (Supplementary ANOVA Table 1). Large seasonal variation in zooplankton biomass was evident in the upstream locations as compared to downstream (Supplementary ANOVA Table 2).

3.9. Segregation of Environmental and Plankton Variables

The result of NMDS/SIMPROF analyses of hydrographical parameters during the Spring Intermonsoon is presented in Fig. 7. Based on the spatial distribution of major physicochemical parameters (salinity, nitrate, phosphate, silicate and dissolved oxygen) during the Spring Intermonsoon, three minor clusters and two major clusters were identified (Fig. 7a & b). The minor clusters 1, 2 and 3 sequentially represented the mesohaline, mesohaline-high saline (polyhaline) and high saline (euhaline) waters in various locations during the time series observations. In subsequent

panels (Fig. 7c –i), the quantitative data of salinity, silicate and plankton food web components are superimposed on spatially clustered time series observations. The quantitative difference in parameters between the mesohaline upstream and euhaline downstream during the Spring Intermonsoon are presented in Fig. 7. It is clear that there was a noticeable increase in the abundance of autotrophic picoplankton, autotrophic nanoplankton, heterotrophic nanoplankton, microzooplankton and mesozooplankton in the upstream mesohaline regions (L3 and L4) as compared to the downstream euhaline region (L1 and L2).

The spatial distribution of hydrographical parameters measured during the Southwest Monsoon segregated using NMDS/SIMPROF has been depicted in Fig. 8. Two major clusters of observations were segregated for the Southwest Monsoon based on the distribution of physicochemical parameters (Fig. 8a and b). The clusters 1 and 2 represented the mesohaline and oligohaline waters, respectively, in various sampling locations during the time series measurements. In the subsequent panels (Fig. 8c –i), the quantitative data of salinity, silicate and plankton food web components are superimposed on spatially clustered time series observations. It was possible in these Figs to distinguish the oligohaline upstream and mesohaline downstream regions during the Southwest Monsoon. The abundance of autotrophic picoplankton, heterotrophic picoplankton, heterotrophic nanoplankton, microzooplankton and mesozooplankton was noticeably high in the downstream mesohaline regions as compared to the upstream oligohaline region.

3.10. Interrelationships of Environmental Parameters and Plankton Components

RDA clearly demarcated the spatial difference and dynamics in environmental parameters during the sampling periods and also presented how they influence the food web components (Fig. 9). The RDA full model in which salinity, silicate, phosphate, dissolved oxygen and nitrate were considered as environmental variables showed that they together explained 52.1% and 57.9% of the variance in plankton components during the Spring Intermonsoon and the Southwest Monsoon, respectively. The RDA partial model, with salinity as the foremost variable and silicate and dissolved oxygen as co-variables, showed that the major variable alone could explain 32% of the variance in biological parameters during both seasons. Monte Carlo test showed that all the ordinations attempted in the RDA analyses are significant ($F = 4.915$, $P = 0.006$ in Spring Intermonsoon and $F = 5.215$, $P = 0.008$ in Spring Intermonsoon) and the noticeable environmental features evidenced in the analyses is summarized below.

The prevalence of high salinity in the downstream sites was evident in the Triplot. During the Spring Intermonsoon, the downstream was polyhaline (18-30) and euhaline (>30) whereas the

upstream was mesohaline (5-18). During the Southwest monsoon, the upstream was limnohaline (<0.5) and oligohaline (0.5-5) and the downstream mesohaline (5-18). An inverse relationship between dissolved oxygen and silicate with salinity was evident as they increased with a decrease in salinity during both seasons. Though the overall pattern during both seasons showed an increasing trend in salinity towards downstream, the salinity values during the Spring Intermonsoon were significantly higher than those observed during the Southwest Monsoon. During both seasons, the upstream region was characterized by higher silicate and dissolved oxygen associated with the river influx whereas the downstream locations had higher phosphate concentration associated with saline waters intrusion. It is clear in RDA that changes in the salinity gradients make a noticeable difference in the distribution of most of the plankton functional components. During the Spring Intermonsoon, autotrophic picoplankton, microzooplankton, heterotrophic nanoplankton and autotrophic nanoplankton increased towards the upstream sites. On the other hand, during the Southwest Monsoon, autotrophic picoplankton, heterotrophic nanoplankton, microzooplankton and mesozooplankton were noticeably high downstream. The total chlorophyll a distribution during both sampling periods did not show any spatial and temporal trend with respect to any of the environmental features.

4. Discussion

4.1. Temporal and Spatial Variations in Hydrography

Being a monsoonal estuary, the CBW is characterized by large seasonal salinity fluctuation caused by the alternating dry (Spring Intermonsoon) and rainy (Southwest Monsoon) periods (Madhupratap 1987; Qasim 2003). The semidiurnal mixed tides play a dominant role in spatial distribution of salinity, in the CBW, during the Spring Intermonsoon whereas large fresh water influx upstream dominates over tidal forcing during the Southwest Monsoon (Srinivas et al. 2003). The maximum tidal height in the CBW observed during the present study was 0.7m during the Spring Intermonsoon period, which indicates the low tidal amplitude/microtidal behavior of the system. The time lag in the tidal phase upstream is a general feature of the CBW due to its vastness, about 50km stretch from the Kochi inlet to the L4 site upstream (Sivaprasad et al. 2013).

During the Spring Intermonsoon, the river influx into the CBW becomes the seasonal lowest, which favors active salinity incursion into the system through the inlets (Qasim2003; Jyothibabu et al. 2006);this, in turn, causes the highest seasonal salinity observed in the CBW during the Spring Intermonsoon. The high nutrient concentration observed throughout the CBW is a typical feature of the system irrespective of seasons (Qasim 2003; Jyothibabu et al. 2006). The five rivers that empty

into the study area are responsible for the high concentration of silicate whereas several non-point sources also contribute to the elevated nitrate levels (Sankaranarayanan and Qasim 1969; Saraladevi et al. 1983; Jyothibabu et al. 2006). The phosphate concentration in the CBW was the seasonal highest during the Spring Intermonsoon due to high salinity during the period, which aids the desorption of phosphate from the suspended particles (Reddy and Sankaranarayanan 1972; Martin et al. 2008). The high concentration of nutrients in the system supported high concentration of chlorophyll irrespective of seasons, indicating that the primary producers were always abundant (Jyothibabu et al. 2006; Madhu et al. 2007). However, chlorophyll did not show any positive correlation with the nitrate and silicate probably due to the exceedingly high concentration of these nutrients present at many stations. During the Spring Intermonsoon, the distribution of physicochemical parameters in most of the study locations showed relatively minor tidal variations whereas the spatial difference between the locations in the downstream and the upstream was large (Fig. 1, Supplementary ANOVA Table 1).

During the Southwest Monsoon, due to heavy rainfall, freshwater occupied a major part of the CBW (Madhupratap et al. 1987; Jyothibabu et al. 2006). This seasonal physiographic feature of the study region was clear in the present study also. Large seasonal variation in salinity was evident in all the study locations (Supplementary ANOVA Table 2). The enormous freshwater influx during the Southwest Monsoon caused low tidal amplitude in the CBW. Due to increased fresh water influx and the resulting low salinity, the concentration of dissolved oxygen in the entire study area was the seasonal highest during the Southwest Monsoon. The nitrate (NO_3) concentration was high during the Southwest Monsoon, contributed both by the river influx and non-point sources (Qasim 2003; Jyothibabu et al. 2006). The silicate (SiO_4) concentration was the seasonal highest during the Southwest Monsoon assisted by the increased river influx during the period. This caused large seasonal fluctuation in the availability of silicate in the CBW (Supplementary ANOVA Table 2). The overall trend in distribution of physicochemical parameters showed low tidal variations of all parameters except the salinity. On the other hand, the spatial variations in most of the hydrographical parameters between the downstream (L1 and L2) and the upstream (L3 and L4) sites were significant (Table 1, Supplementary ANOVA Table 2).

Most of the hydrographical parameters during both seasons showed minor tidal variations as compared to their spatial and seasonal variations. Low tidal variations of the physicochemical parameters in most of the study locations can be attributed to the low tidal amplitude in the system. The study showed that, during the Spring Intermonsoon, the downstream region was polyhaline (18-30) and euhaline (>30) whereas the upstream area was mesohaline (5-18). During the Southwest

Monsoon, the upstream was limnohaline (<0.5) and oligohaline (0.5-5) and the downstream mesohaline (5-18). These spatial shifts in salinity regimes during the two seasonal samplings caused changes in the distribution of biological components. The autotrophic picoplankton, heterotrophic nanoplankton, microzooplankton and mesozooplankton showed a clear seasonal shift from the upstream during the Spring Intermonsoon to the downstream during the Southwest Monsoon. This indicates the spatial shift in the abundance of planktonic grazers in the CBW during the two seasons. Conversely, irrespective of seasons, the autotrophic nanoplankton was higher in the upstream.

4.2. Ecology and Dynamics of the Plankton Food Web

The present study exhibited that both autotrophic and heterotrophic forms of pico and nanoplankton are abundant in monsoonal estuaries. As mentioned earlier, the trophic interaction in a plankton food web becomes effective when both prey and consumers become abundant and coexists in time and space (Landry and Fagerness 1988; Landry et al. 2008; Garrison et al. 2000; Calbert 2004). During the Spring Intermonsoon, all plankton components, especially the consumers, were much more abundant than during the Southwest Monsoon. Consequently, each interaction between different prey-predator pairs occurred effectively, resulting into efficient functioning of the plankton food web. The existence of a strong plankton food web provides high substrate availability for higher trophic levels (Landry et al. 1988, 2008; Jyothibabu et al. 2006). While considering the spatial distribution of plankton components in the CBW during the Spring Intermonsoon, the upstream mesohaline regions seem to have a more efficient plankton food web as compared to the downstream due to close coupling between plankton consumers and their potential prey.

The hydrography of the CBW changes drastically during the Southwest Monsoon due to enormous fresh water influx from rivers that feed the upstream region (Madhupratap et al. 1987). This hydrographical ramification disturbs the coexistence of prey and consumers in the CBW. It is very evident in Table 1 that the abundance of all plankton food web components in the CBW was low during the Southwest Monsoon suggesting a weak plankton food web during the period. The present study also emphasizes the drop in consumer abundance in the upstream locations during the Southwest Monsoon, which makes the spatial distribution of predator and prey discrete. For example, it has been proved that heterotrophic nanoplankton predominantly feeds on bacteria (Fenchel 1982 a & b; Hass et al. 1982). However, during the Southwest Monsoon, though heterotrophic picoplankton was present in the oligohaline upstream in the CBW, their predator population, heterotrophic nanoplankton, was largely concentrated in the mesohaline downstream sites. Similarly, the low abundance of microzooplankton in the upstream region during the Southwest

Monsoon causes not only the inefficient utilization of heterotrophic nanoplankton, but autotrophic pico and nanoplankton also (Sherr et al. 1991; Bernad and Rassoulzadagan 1993; Verity 1986).

The high heterotrophic picoplankton abundance and production in the CBW is a major carbon source to support an efficient microbial food web in the system (Thottathil et al. 2008a). The present study shows that during the Southwest Monsoon, the heterotrophic picoplankton biomass in the upstream sites is probably being grazed less efficiently by the heterotrophic nanoplankton due to the spatial disparity in their distribution. Sherr and Sherr (1994) showed that heterotrophic nanoplankton is the dominant grazer of both heterotrophic and autotrophic picoplankton in the marine environment. In the present observation, a significant positive correlation was observed between autotrophic picoplankton and heterotrophic nanoplankton during the Spring Intermonsoon. Experiments specify that heterotrophic nanoplankton are capable of growing as fast as or even faster than the autotrophic picoplankton (Goldman 1985). On the other hand, during the Southwest Monsoon, significantly low abundance of heterotrophic nanoplankton and microzooplankton in the upstream sites potentially causes a weak transfer of autotrophic and heterotrophic picoplankton carbon to the higher trophic levels.

The dominance of *Tintinnopsis* found in the in the microzooplankton community of the CBW is a typical feature of the estuarine system as they require mineral flakes plentiful in the estuaries to construct their lorica (Jyothibabu et al. 2006). The mesozooplankton biomass and abundance in the CBW are markedly low during the Southwest Monsoon (Wellershaus 1974; Madhupratap 1987). In addition to weak plankton food web and osmotic imbalances during the Southwest Monsoon, the high flushing rate of the CBW also can contribute to the low zooplankton biomass during the period. The flushing rate of the CBW is 5-7 times faster during the Southwest Monsoon as compared to the Spring Intermonsoon (Shivaprasad et al. 2013). Due to large freshwater influx and faster flushing during the Southwest Monsoon, the mesozooplankton present upstream of the CBW would be washed down to the downstream locations. This condition lasts for some time, but it is too short a period for the development of a low saline-adapted zooplankton community in the downstream sites, which cause a sparse zooplankton community in the CBW during the SWM period (Wellershaus 1974; Madhupratap 1987).

Spatial difference and segregation in plankton food web components were very clear in the CBW during both sampling periods. During the Spring Intermonsoon, autotrophic picoplankton, autotrophic nanoplankton, heterotrophic nanoplankton and microzooplankton increased towards the upstream where mesohaline conditions prevailed. On the other hand, during the Southwest Monsoon,

autotrophic picoplankton, heterotrophic picoplankton, heterotrophic nanoplankton, microzooplankton and mesozooplankton increased noticeably downstream where mesohaline conditions prevailed. This indicates a clear spatial shift in the region of efficient plankton food web in the CBW during the two seasons, which will have applications in designing the seasonal food web models for monsoonal estuaries.

5. Conclusion

Based on a time series measurement along the salinity gradients, this study presents the ecology and seasonal dynamics of various plankton food web components in the CBW. The study showed that the spatial and seasonal variations in plankton food web components are more significant than that caused by tidal action. The plankton food web in the CBW was found to be more efficient during the spring Intermonsoon period as there was high abundance of all the prey components and their consumers. Spatially, the plankton trophic interactions in the CBW during the Spring Intermonsoon was more efficient upstream (mesohaline) where there was a close coupling between all prey components and their consumers. On the other hand, during the Southwest Monsoon, the plankton food web was more effective downstream (mesohaline) regions where all plankton consumers were significantly high. Statistical analyses confirmed that a more efficient plankton food web in CBW exist in the mesohaline regions during both seasons and suggests a spatial shift of active plankton food web region from the upstream during the Spring Intermonsoon to the downstream during the Southwest Monsoon.

Acknowledgement

The authors thank the Director, CSIR- National Institute of Oceanography, India for facilities and encouragement. We thank all CSIR - NIO staff who helped to carry out the simultaneous time series measurements in the Cochin backwaters. The authors thank ICMAM-PD, Chennai for financial support for the Grant-in-Aid project 'Ecosystem modeling of Cochin backwaters' funded by ICMAM – PD Chennai. This is NIO contribution XXXX.

References

- Azam, F.T., Fenchel, J.G., Field, J.S., Gray, L.A., Meyer-Reil & Thingstad, F. (1983). The ecological role of water-column microbes in the sea. *Marine Ecology Progress Series*, 1, 257-263.
- Bernard, C. & Rassoulzadegan, F. (1993). The role of picoplankton (cyanobacteria and plastidic picoflagellates) in the diet of tintinnids. *Journal of Plankton Research*, 15, 361-373.
- Birks, H.J.B. (1998). Numerical tools in palaeolimnology -Progress, potentialities and problems. *Journal of Paleolimnology*, 20, 307 - 332.

- Bloem, J., Marie-Jos, Bär-Gilissen, M. & Cappenberg, T.E. (1986). Fixation, Counting, and Manipulation of Heterotrophic Nanoflagellates. *Applied and Environmental Microbiology*, 52, 1266-1272.
- Calbet, A. & Landry, M.R. (2004). Phytoplankton growth, microzooplankton grazing, and carbon cycling in marine systems. *Limnology and Oceanography*, 40, 51-57.
- Clarke, K.R. & Warwick, R.M. (2001). *Changes in Marine Communities: An Approach to Statistical Analysis and Interpretation*, Plymouth: Plymouth Marine Laboratory, Primer E limited, UK, PP. 176
- Fenchel, T. (1982a). Ecology of heterotrophic microflagellates. II. Bioenergetics and growth. *Marine Ecology Progress Series*, 8, 225-231.
- Fenchel, T. (1982b). Ecology of heterotrophic microflagellates IV. Quantitative occurrence and importance as consumers of bacteria. *Marine Ecology Progress Series*, 9, 35-62.
- Garrison, D.L., Gowing, M.M., Hughes, M.P., Campbell, L., Caron, D.A., Dennett, M.R., Shalapyonok, A., Olson, R.J., Landry, M.R., Brown, S.L., Liu, H.-B., Azam, F., Steward, G.F., Ducklow, H.W. & Smith, D.C. (2000). Microbial food web structure in the Arabian Sea: a US JGOFS study. *Deep Sea Research Part II: Topical Studies in Oceanography*, 47, 1387-1422.
- Goldman, J.C. & Caron, D.A. (1985). Experimental studies on an omnivorous microflagellate: implications for grazing and nutrient regeneration in the marine microbial food chain. *Deep Sea Research Part A Oceanographic Research Papers*, 32, 899-915.
- Grasshoff K, Ehrhardt M & K., K. (1983). Methods of Seawater Analysis. *In: Grasshoff K, Ehrhardt M, Kremling K editors, Verlag Chemie, Weinheim*, 89 – 224.
- Haas, L.W. (1982). Improved epifluorescence microscopy for observing planktonic microorganisms. *Annales Institute of Oceanography, Paris*, 58, 261-266.
- Harris, R.P., Wiebe, J., Lenz, H.R., Skjoldal, M.E. & Huntley (2000). *ICES Zooplankton Methodology Manual*, London: Academic Press, PP.
- Iriarte, A. & Purdie, D.A. (1994). Size distribution of chlorophyll a biomass and primary production in a temperate estuary (Southampton Water): the contribution of photosynthetic picoplankton. *Marine Ecology Progress Series*, 115, 283-297.
- Jyothibabu, R., Madhu, N.V., Jayalakshmi, K.V., Balachandran, K.K., Shiyas, C.A., Martin, G.D. & Nair, K.K.C. (2006). Impact of freshwater influx on microzooplankton mediated food web in a tropical estuary (Cochin backwaters e India). *Estuaries and Coastal Shelf Science*, 69, 505 – 518.
- Kimmerer, W.J., Burau, J.R. & Bennett, W.A. (1998). Tidally oriented vertical migration and position maintenance of zooplankton in a temperate estuary. *Limnology and Oceanography*, 43, 1697-1709.
- Kofoed, C.A. & Canmpbell, A.S. (1939). Reports on the scientific results of the expedition to the Eastern Tropical Pacific, in charge of Alexander Agassiz, US Fish Commission steamer “Albatross”, from October 1904 to March 1905. *University California Publications in Zoology*, 34, 1 - 403.
- Krishnamurty, K., Naidu, D.W., Godhantaraman, N., Kannan, L. & Kathiresan K. (1995). Microzooplankton with special reference to Tintinnida (Protozoa:Ciliata: Tintinnida). Plankton of Pangipettai (Porto Novo), India. *Fasicle No1, New Series: Memoirs of the centre for advanced study in Marine Biology, (Annamalai University), Parangipettai, Tamilnadu, India: 27.*
- Landry, M.R., Decima, M., Simmons, M.P., Hannides, C.C.S. & Daniels, E. (2008). Mesozooplankton biomass and grazing responses to Cyclone Opal, a subtropical mesoscale eddy. *Deep Sea Research Part II: Topical Studies in Oceanography*, 55, 1378-1388.

- Landry, M.R. & Fagerness, V.L. (1988). Behavioral and morphological influences on predatory interactions among marine copepods. *Bulletin of Marine Science*, 43, 509-529.
- Lee, C.Y., Liu, D.C. & Su, W.C. (2009). Seasonal and Spatial Variations in the Planktonic Copepod Community of Ilan Bay and Adjacent Kuroshio Waters off Northeastern Taiwan. *Zoological Studies*, 48, 151-161.
- Leps, J. & Smilauer, P. (2003). *Multivariate Analysis of Ecological Data using CANOCO*: Cambridge University Press.
- Lin, D., Li, X.Q., Fang, H.D., Dong, Y.H., Huang, Z.X. & Chen, J.H. (2011). Calanoid copepods assemblages in Pearl River Estuary of China in summer: Relationships between species distribution and environmental variables. *Estuarine Coastal and Shelf Science*, 93, 259-267.
- Madhu, N.V., Jyothibabu, R., Balachandran, K.K., Honey, U.K., Martin, G.D., Vijay, J.G., Shiyas, C.A., Gupta, G.V.M. & Achuthankutty, C.T. (2007). Monsoonal impact on planktonic standing stock and abundance in a tropical estuary (Cochin backwaters - India). *Estuarine, Coastal and Shelf Science*, 73, 54-64.
- Madhupratap, M. & Rao, T.S.S. (1979). Tidal and Diurnal Influence on Estuarine Zooplankton. *Indian Journal of Marine Sciences*, 8, 9-11.
- Madhupratap, M., Nair, V.R., Nair, S.R.S. & Achuthankutty, C.T. (1981). Zooplankton abundance of the Andaman Sea. *Indian Journal of Marine Sciences*, 10, 258-261.
- Madhupratap, M. (1987). Status and strategy zooplankton of tropical Indian estuaries: a review. *Bulletin of Plankton Society of Japan*, 65-81.
- Maeda, M. (1986). An illustrated guide to the species of the Family Halteridae and Strombilidae (Oligotrichida, Ciliophora), free swimming protozoa common in the aquatic environments. (eds. Asai, T., Kobayashi, K., Sakai, H., Nemoto, T., Kajihara, T) *Ocean Research Institute University of Tokyo*, 21, 67
- Martin, G.D., Vijay, J.G., Laluraj, C.M., Madhu, N.V., Joseph, T., Nair, M., Gupta, G.V.M. & Balachandran, K.K. (2008). Fresh water influence on nutrient stoichiometry in a tropical estuary, Southwest coast of India. *Applied Ecology Environmental Research*, 6, 57-64.
- Menon, N.N., Balchand, A.N. & Menon, N.R. (2000). Hydrobiology of the Cochin backwater system – a review. *Hydrobiologia*, 430, 149 – 183.
- Porter, K.G. & Feig, Y.S. (1980). The use of DAPI for identifying and counting aquatic microflora. *Limnology and Oceanography*, 25, 943-948.
- Qasim, S.Z. (2003). Indian Estuaries (Allied publication Pvt. Ltd. Heredia Marg, Ballard estate, Mumbai). Pp. 259.
- Ram, A.S.P., Nair, S. & Chandramohan, D. (2003). Seasonal shift in net ecosystem production in a tropical estuary. *Limnology and Oceanography*, 48, 1601-1607.
- Reddy, C.V.G. & Sankaranarayanan, V.N. (1972). Phosphate regenerative activity in the muds of a tropical estuary. *Indian Journal of Marine Sciences*, 1, 57-60.
- Sankaranarayanan, V.N. & Qasim, S.Z. (1969). Nutrients of the Cochin Backwater in relation to environmental characteristics. *Marine Biology*, 2, 236-247.
- Sankaranarayanan, V.N., Udaya, V.P., Balachandran, K.K., Pylee, A.J. & Joseph, T. (1986). Estuarine characteristics of a lower reaches of the river Periyar (Cochin backwaters). *Indian Journal of Marine Sciences*, 1, 166-170.

- Saraladevi, K., Venugopal, P., Remani, K.N., Zacharias, D. & Unnithan, R.V. (1983). Nutrients in some estuaries of Kerala. *Mahasagar – The Bulletin of National Institute of Oceanography, Goa*, 16, 161 – 173.
- Sherr, E.B., Sherr, B.F., Berman, T. & Hadas, O. (1991). High abundance of picoplankton-ingesting ciliates during late fall in Lake Kinneret, Israel. *Journal of Plankton Research*, 13, 789-799.
- Sherr, E.B. & Sherr, B.F. (1994). Bacterivory and herbivory: Key roles of phagotrophic protists in pelagic food webs. *Microbial Ecology*, 28, 223-235.
- Shivaprasad, A., Vinita, J., Revichandran, C., Reny, P.D., Deepak, M.P., Muraleedharan, K.R. & Naveen Kumar, K.R. (2013). Seasonal stratification and property distributions in a tropical estuary (Cochin estuary, west coast, India). *Hydrology and Earth System Sciences*, 17, 187-199.
- Srinivas, K., Revichandran, C., Maheswaran, P.A., Mohamed, T.T.A. & Murukesh, N. (2003). Propagation of tides in the Cochin estuarine system, southwest coast of India. *Indian Journal of Marine Sciences*, 32, 14-24.
- Subrahmanyam, R. (1971). *The Dinophyceae of the Indian Seas, Memoir II, Part 2, Family Peridineacea*, Marine Biological Association of India, Cochin, India.
- Thottathil, S.D., Balachandran, K.K., Gupta, G.V.M., Madhu, N.V. & Nair, S. (2008a). Influence of allochthonous input on autotrophic-heterotrophic switch-over in shallow waters of a tropical estuary (Cochin Estuary), India. *Estuarine Coastal Shelf Science*, 78, 551-562.
- Thottathil, S.D., Balachandran, K.K., Jayalakshmy, K.V., Gupta, G.V.M. & Nair, S. (2008 b). Tidal switch on metabolic activity: Salinity induced responses on bacterioplankton metabolic capabilities in a tropical estuary. *Estuarine, Coastal and Shelf Science*, 78, 665-673.
- UNESCO (1994). Protocols for the Joint Global Ocean Flux Study. *Manual and Guides*, 29, 170.
- Verity, P.G. (1986). Grazing on phototrophic nanoplankton by microzooplankton in the Narragansett Bay, Rhode Island. *Marine Ecology Progress Series*, 29, 105-115.
- Vijith, V., Sundar, D. & Shetye, S.R. (2009). Time-dependence of salinity in monsoonal estuaries. *Estuarine, Coastal and Shelf Science*, 85, 601-608.
- Wellershaus, S. (1974). Seasonal changes in the zooplankton population in the Cochin Backwater (a South Indian estuary). *Hydrobiological Bulletin*, 8, 213-223.
- Yang, G.M., Dh He, Wang, C.S., Miao, Y.T. & Yu, H.H. (1999). Study on the biological oceanography characteristics of planktonic copepods in the waters north of Taiwan, II. Community characteristics. *Acta Oceanologica sinica*, 21, 72-80.

Figure Captions

Figure 1 - The study area (Cochin Backwaters) with the time series locations indicated in red circles. Azhikode (L1) and Kochi (L2) were situated in downstream, whereas, Arookutty (L3) and Thannermukkom (L4) were in upstream. Three hourly time series measurements were carried out in these locations for 24 hours during the Spring Intermonsoon (dry season) and Southwest Monsoon (wet season).

Figure 2 - Distribution of physicochemical variables in the Cochin Backwaters during the Spring Intermonsoon. The panel (a) shows the variation in tidal height during the observation and panel (b) represents the salinity variation with respect to the tidal phase. The salinity distribution is set as the background in subsequent panels with white contour lines representing (c) dissolved oxygen (DO), (d) nitrate (NO_3), (e) phosphate (PO_4) and (f) silicate (SiO_4).

Figure 3 - Distribution of physicochemical variables in the Cochin Backwaters during the Southwest Monsoon. The panel (a) shows the variation in tidal height during the observation and panel (b) represents the salinity variation with respect to the tidal phase. The salinity distribution is set as the background in subsequent panels with white contour lines representing (c) dissolved oxygen (DO), (d) nitrate (NO_3), (e) phosphate (PO_4) and (f) silicate (SiO_4).

Figure 4 - (a) Schematic diagram of the plankton food web in the Cochin backwaters. The subsequent panels represent the photomicrographs of (b) APP - Autotrophic picoplankton, (c) HPP - Heterotrophic Picoplankton, (d) ANP - Autotrophic Nanoplankton, (e) HNP - Heterotrophic Nanoplankton, (f) MZP - Microzooplankton and (g) MSP - Mesozooplankton/copepods. Other abbreviations: AMP- Autotrophic Microplankton and DOC – Dissolved Organic Carbon.

Figure 5 - Spatial distribution of functional components in the plankton food web during the Spring Intermonsoon. The salinity distribution is set as the background in all panels with white circles representing the distribution of (a) APP - Autotrophic Picoplankton ($\times 10^7 \text{ No. L}^{-1}$), (b) ANP - Autotrophic Nanoplankton ($\times 10^7 \text{ No. L}^{-1}$), (c) HPP - Heterotrophic Picoplankton ($\times 10^9 \text{ No. L}^{-1}$) (d) HNP - Heterotrophic Nanoplankton ($\times 10^6 \text{ No. L}^{-1}$) (e) MZP - Microzooplankton ($\times 10^4 \text{ No. L}^{-1}$) and (f) MSP - Mesozooplankton biomass ($\text{ml } 100\text{m}^{-3}$).

Figure 6 - Spatial distribution of functional components in the plankton food web during the Southwest Monsoon. The salinity distribution is set as the background in all panels with white circles representing the distribution of (a) APP - Autotrophic Picoplankton ($\times 10^7 \text{ No. L}^{-1}$), (b) ANP - Autotrophic Nanoplankton ($\times 10^7 \text{ No. L}^{-1}$), (c) HPP - Heterotrophic Picoplankton ($\times 10^9 \text{ No. L}^{-1}$) (d)

HNP - Heterotrophic Nanoplankton ($\times 10^6$ No. L^{-1}) (e) MZP - Microzooplankton ($\times 10^4$ No. L^{-1}) and (f) MSP - Mesozooplankton biomass ($ml\ 100m^{-3}$).

Figure 7 - (a) Cluster and (b) NMDS plots presenting the segregation of locations/observations based on the distribution of physicochemical parameters during the Spring Intermonsoon. The subsequent panels show physicochemical NMDS plots overlaid with the bubbles of (c) salinity, (d) silicate, (e) APP - Autotrophic Picoplankton, (f) ANP - Autotrophic Nanoplankton, (g) HPP - Heterotrophic Picoplankton, (h) HNP - Heterotrophic Nanoplankton (i) MZP - Microzooplankton and (j) MSP - Mesozooplankton for visualizing their distribution based on spatially assembled observations. Abbreviations and unit of measurements are the same as in figure 4&5.

Figure 8 - (a) Cluster and (b) NMDS plots presenting the segregation of locations/observations based on the distribution of physicochemical parameters during the Southwest Monsoon. The subsequent panels show physicochemical NMDS plots overlaid with the bubbles of (c) salinity, (d) silicate, (e) APP - Autotrophic Picoplankton, (f) ANP - Autotrophic Nanoplankton, (g) HPP - Heterotrophic Picoplankton, (h) HNP - Heterotrophic Nanoplankton (i) MZP - Microzooplankton and (j) MSP - Mesozooplankton for visualizing their distribution based on spatially assembled observations. Abbreviations and unit of measurements are the same as in figure 4&5.

Figure 9 - RDA Triplot showing the distribution and interrelationships of environmental and biological parameters during the (a) Spring Intermonsoon and (b) Southwest Monsoon. The overlaid attribution contours (pink dotted line and values) represent the spatial distribution of salinity and its relationship with other environmental and biological components. The sampling locations (1-4) and the time series observations in each of this locations are displayed by small red filled circles. For example points 1.1 -1.9 represent the 9 time series observations carried out at location 1. Different plankton functional components and environmental parameters are displayed by arrows; the blue dotted arrows indicate the former and the black arrows indicate the latter.



Figure 1

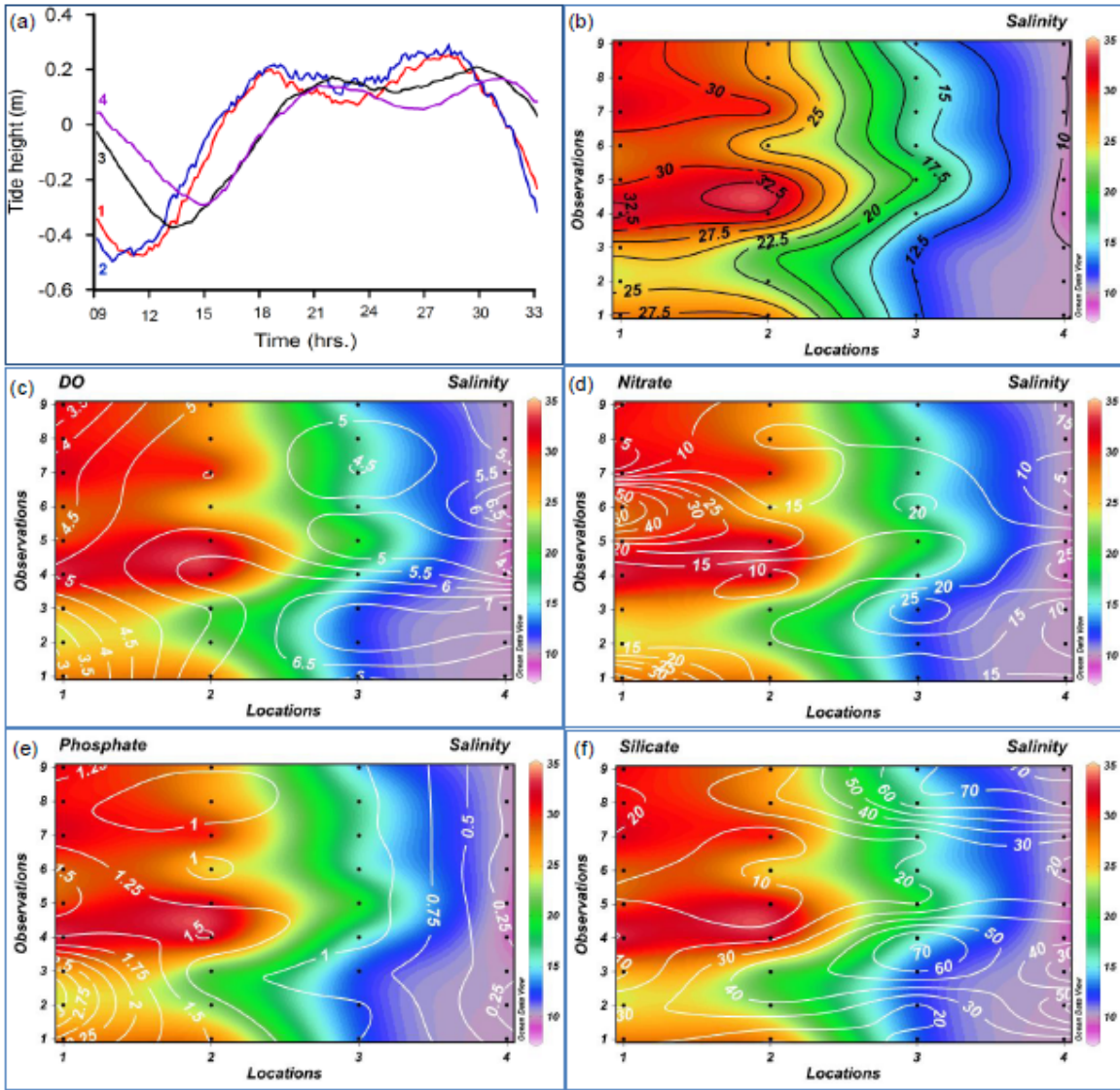


Figure 2

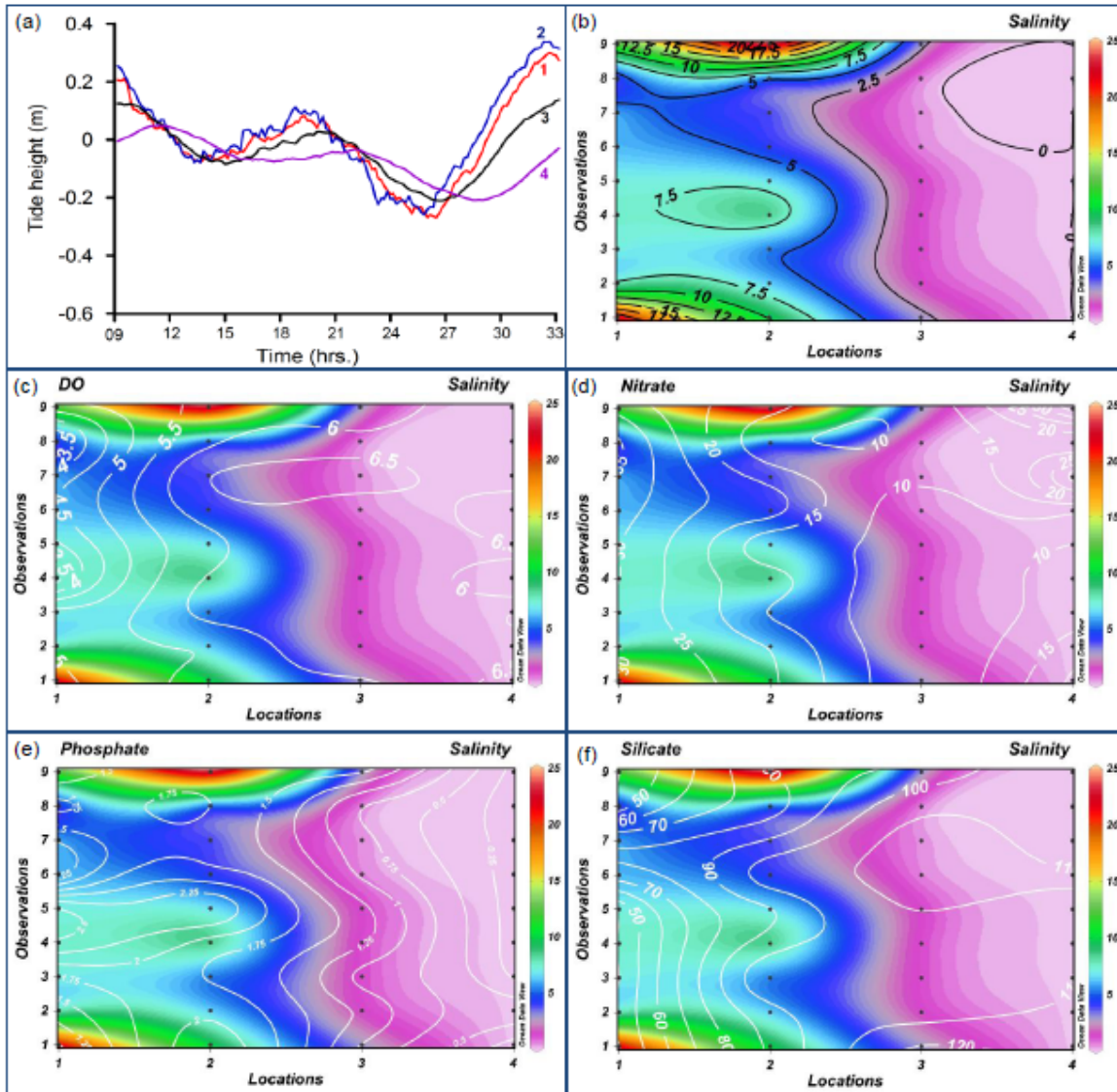


Figure 3

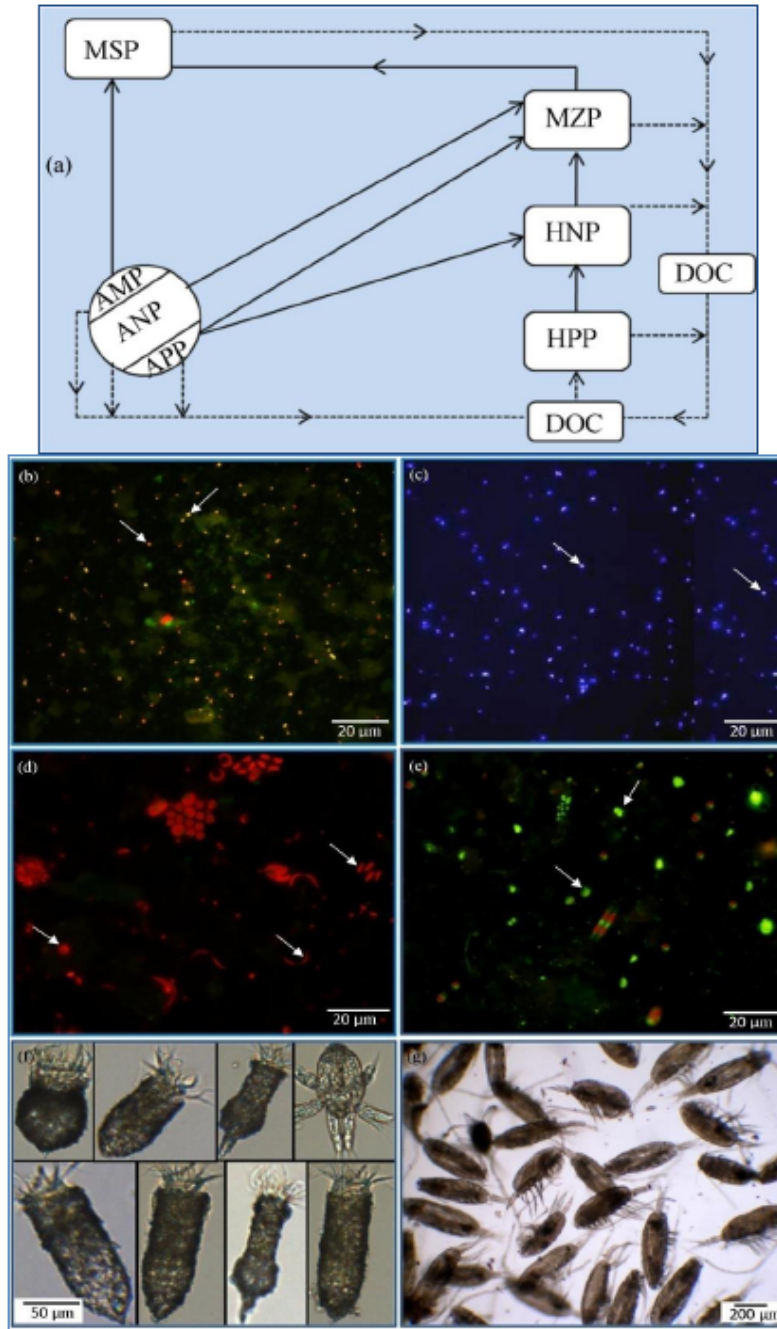


Figure 4

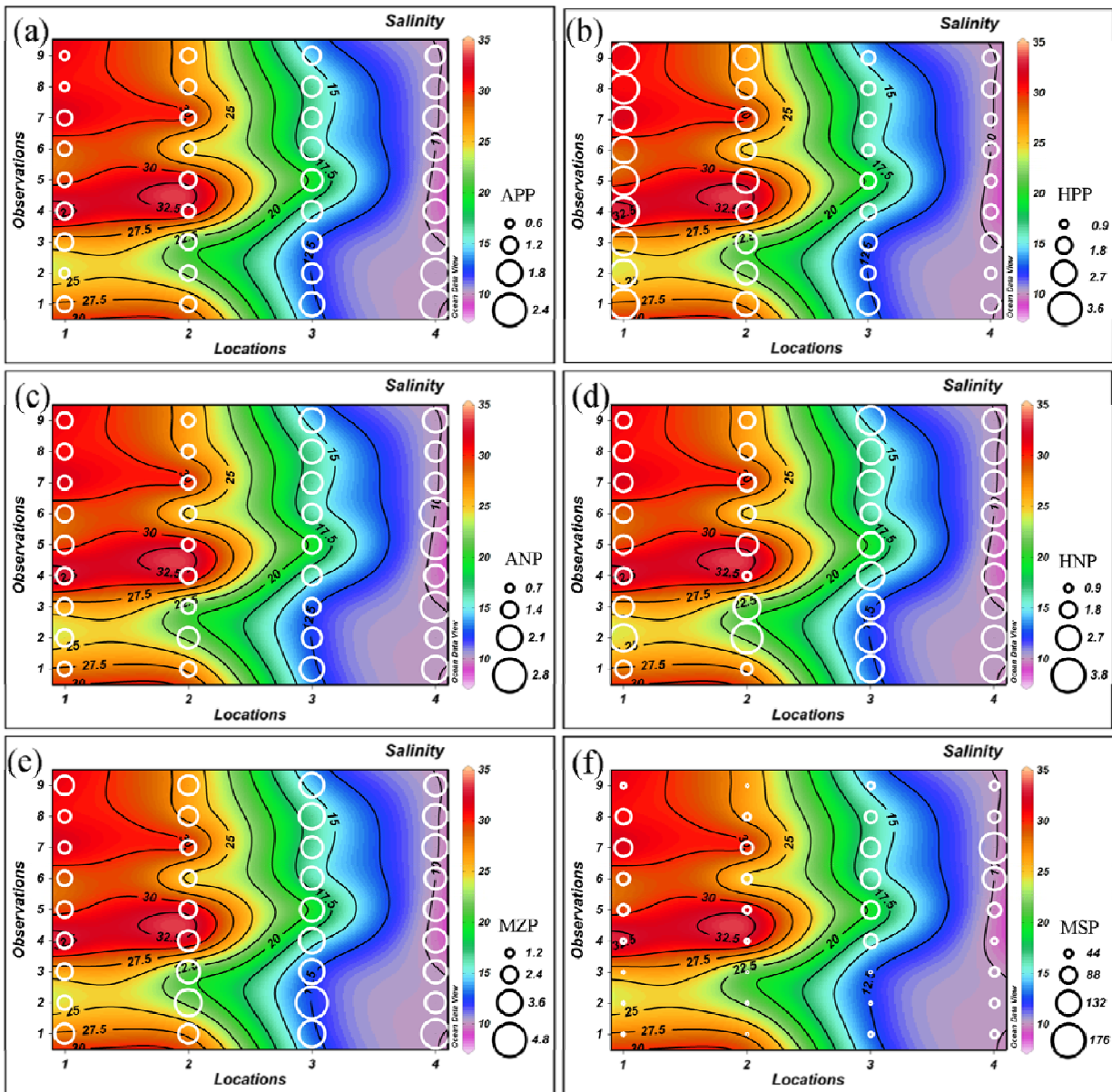


Figure 5

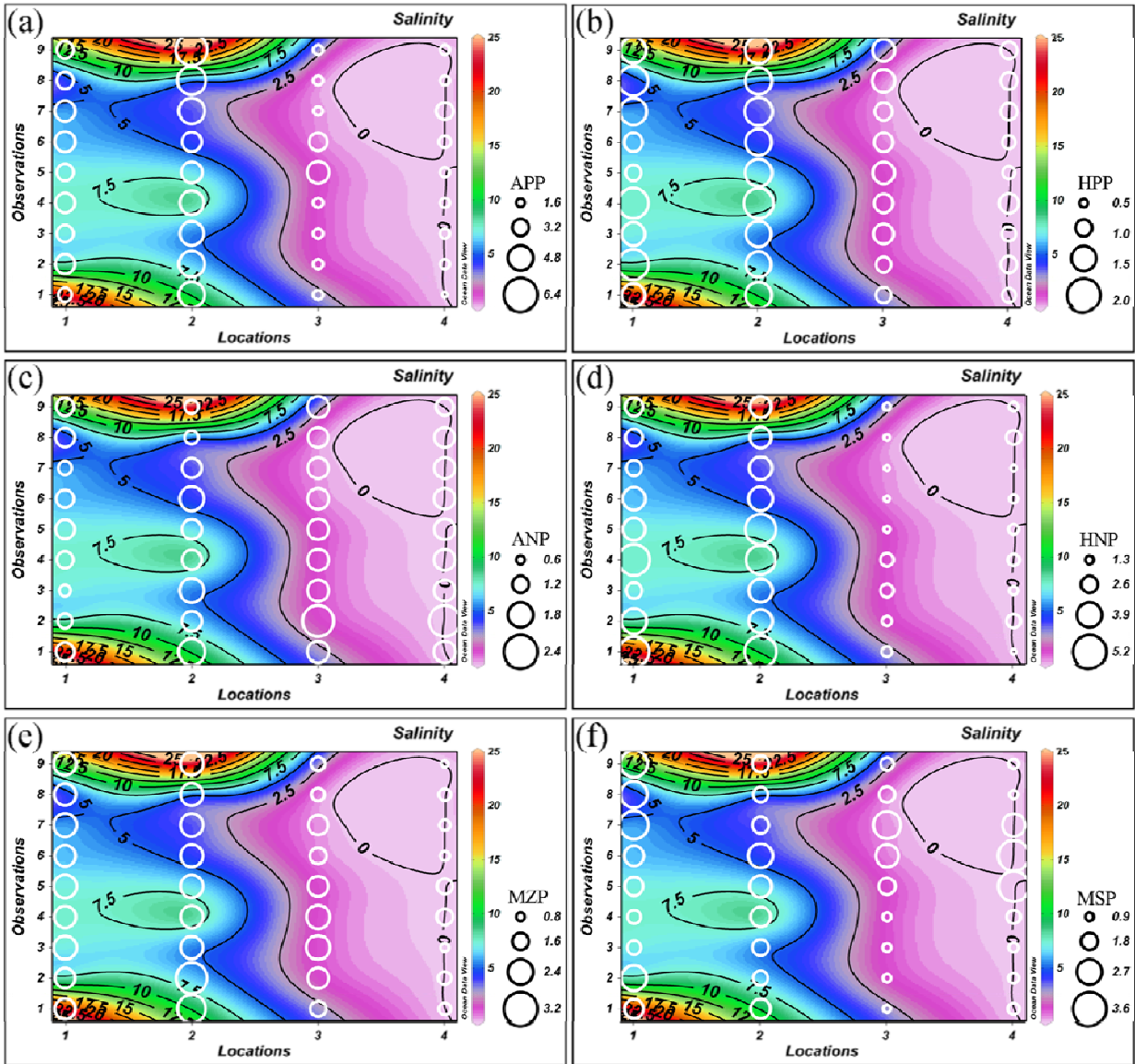


Figure 6

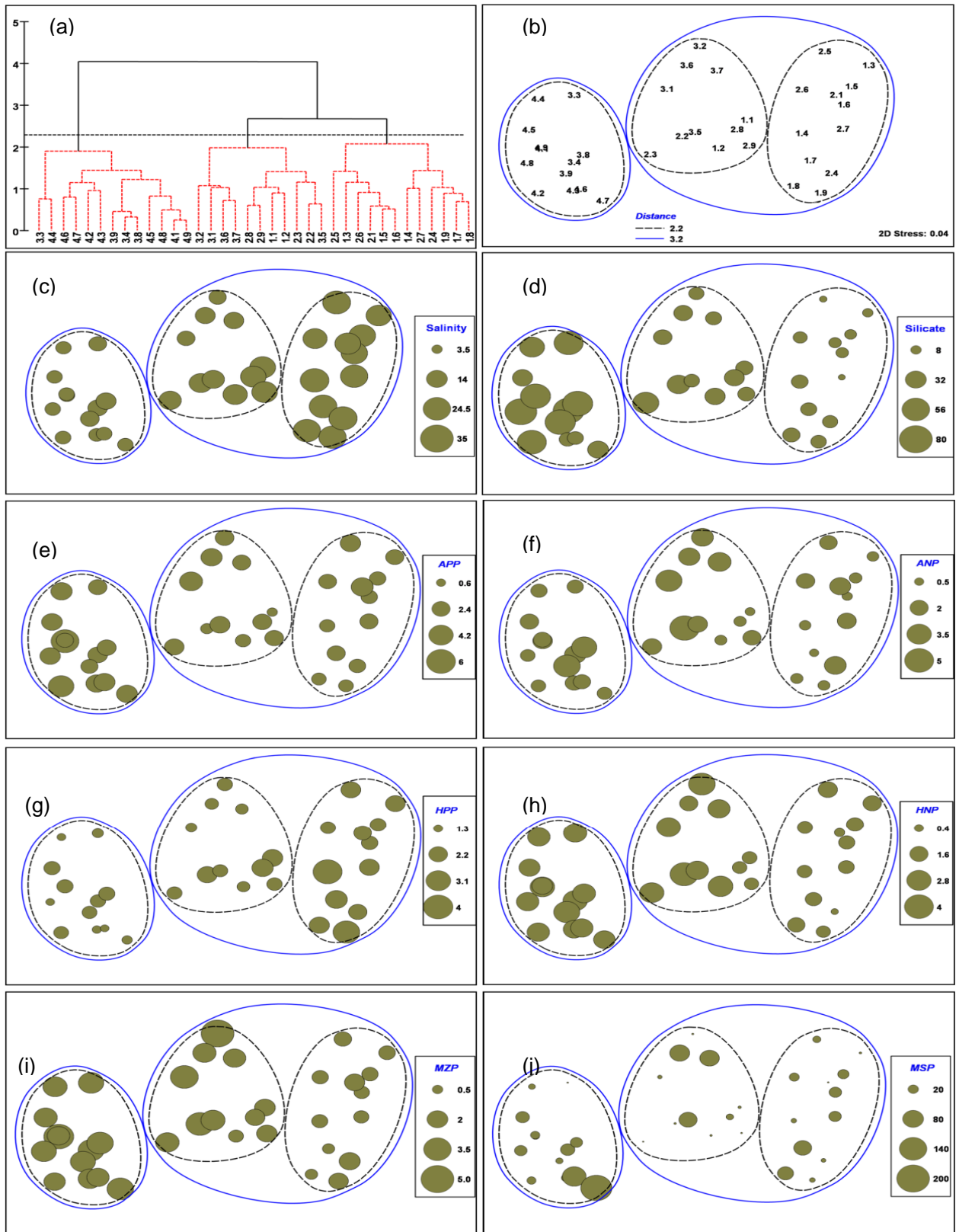


Figure 7

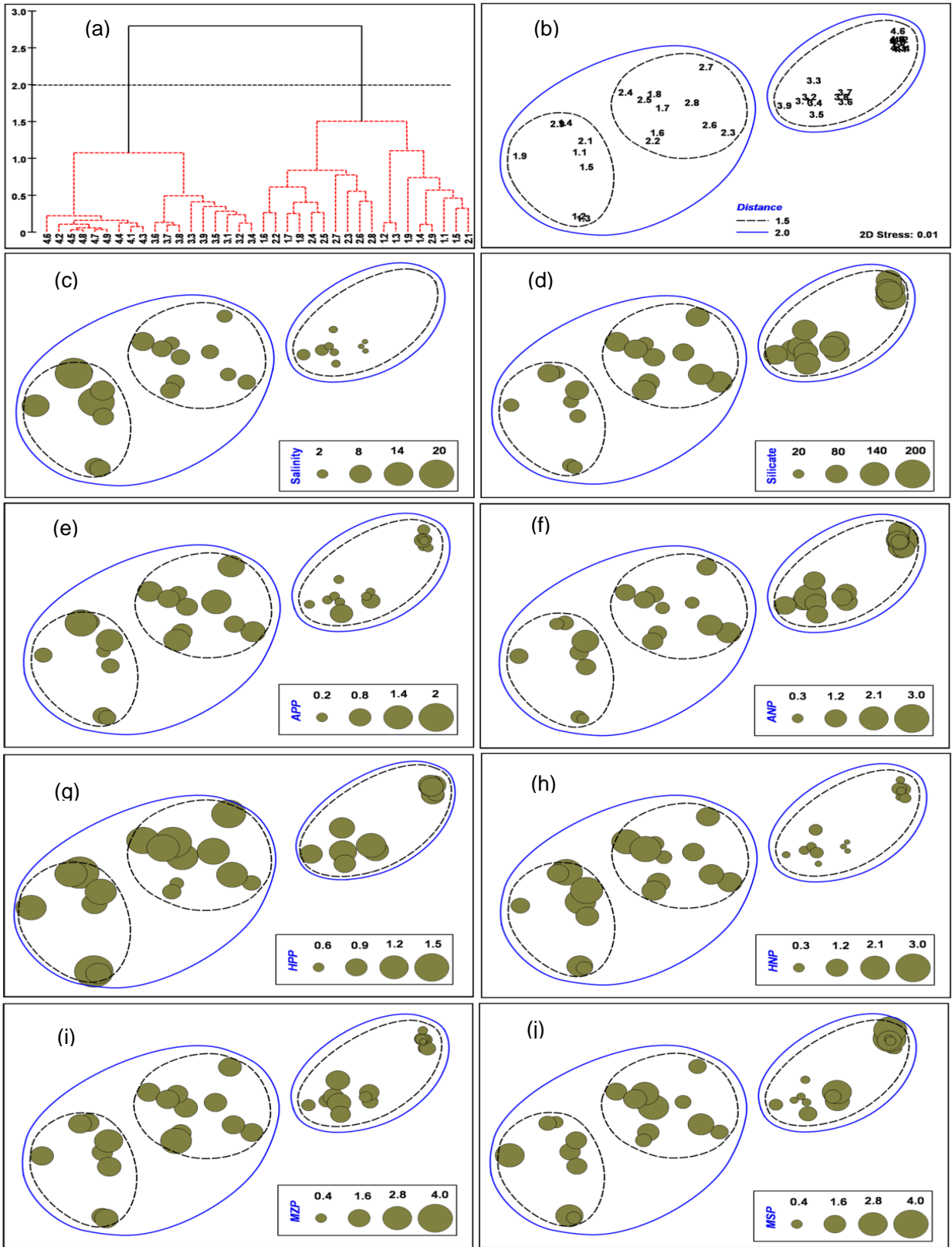


Figure 8

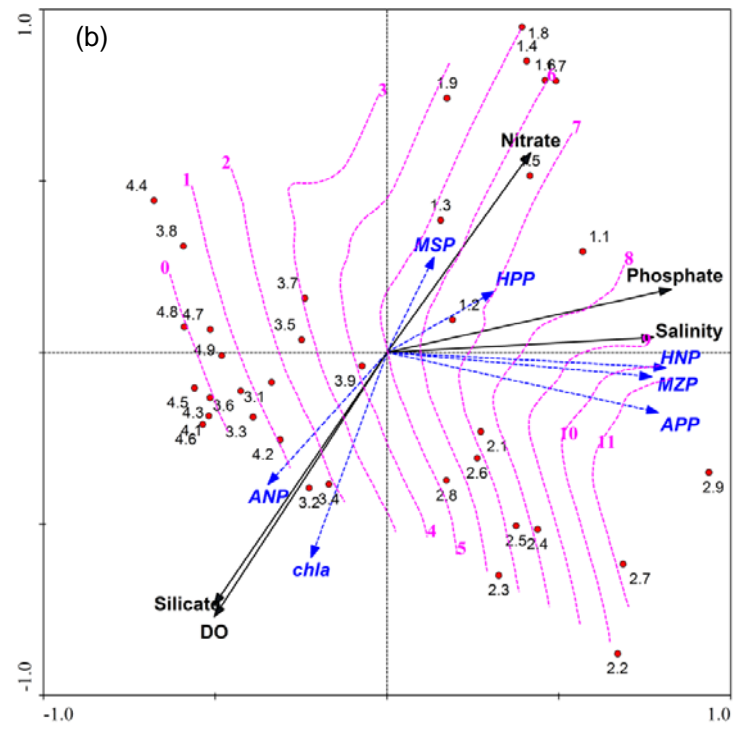
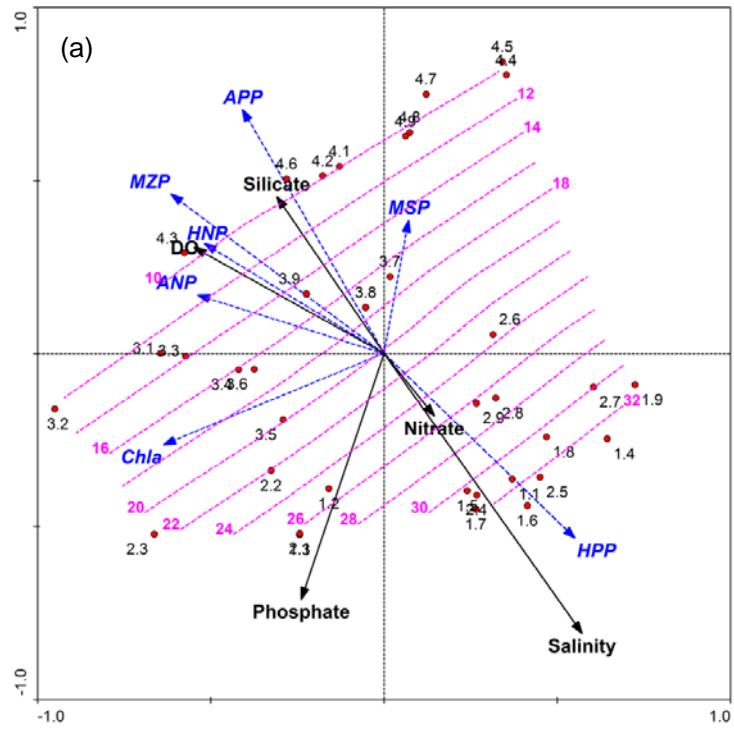


Figure 9

Parameters	Spring Intermonsoon (SIM)				Southwest Monsoon (SWM)			
	L 1	L 2	L 3	L 4	L 1	L 2	L 3	L 4
Salinity	29.15 (0.10)	26.90 (0.15)	15.21 (0.16)	9.99 (0.02)	8.62 (0.60)*	8.66 (0.70)*	2.11 (0.91)*	0.10 (0.30)
DO (mg L ⁻¹)	3.87 (0.15)	5.61 (0.07)	5.58 (0.19)	5.96 (0.15)	4.23 (0.30)	5.83 (0.06)	5.99 (0.06)	6.36 (0.06)
NO ₃ (μM)	16.93 (0.68)*	14.21 (0.35)	16.44 (0.35)	13.42 (0.53)	31.30 (0.08)	16.81 (0.25)	8.74 (0.23)	18.77 (0.51)
PO ₄ (μM)	1.60 (0.59)*	1.44 (0.66)*	1.05 (0.26)	0.23 (0.32)	1.40 (0.40)	1.11 (0.25)	0.60 (0.24)	0.20 (0.80)
SiO ₄ (μM)	17.70 (0.39)	20.90 (0.73)*	40.80 (0.59)*	40.99 (0.50)	42.79 (0.07)	92.62 (0.12)	105.67 (0.08)	108.66 (0.27)
Chl. <i>a</i> (mg m ⁻³)	3.99 (0.45)	9.28 (0.98)*	18.46 (0.99)*	5.91 (0.30)	3.23 (0.80)*	6.52 (0.35)	6.55 (0.72)*	5.55 (0.34)
Density (No.L⁻¹)								
APP (x10 ⁷)	1.80 (0.59)*	2.46 (0.34)	2.73 (0.48)	3.46 (0.28)	1.21 (0.24)	1.52 (0.47)	0.40 (0.28)	0.20 (0.14)
HPP (x 10 ⁸)	2.20 (0.64)*	2.14 (0.61)*	1.75 (0.44)	1.53 (0.39)	1.24 (0.76)*	1.26 (0.61)*	0.86 (0.42)	0.80 (0.31)
ANP (x 10 ⁷)	0.76 (0.33)	2.40 (0.66)*	3.02 (0.63)*	2.8 (0.50)	0.73 (0.30)	1.69 (0.31)	1.52 (0.57)	1.36 (0.40)
HNP (x 10 ⁸)	1.64 (0.46)	1.26 (1.03)*	2.60 (0.20)	2.20 (0.10)	1.10 (0.43)	1.25 (0.50)	0.43 (0.67)*	0.55 (0.60)*
MZP (x 10 ⁸)	1.11 (0.29)	1.93 (0.38)	3.11 (0.25)	2.62 (0.27)	1.98 (0.28)	1.64 (0.11)	1.19 (0.42)	0.48 (0.50)
Biomass (mg C m⁻³)								
APP	4.50 (0.59)*	6.15 (0.34)	6.83 (0.48)	8.65 (0.28)	0.21 (0.24)	0.25 (0.47)	0.15 (0.28)	0.10 (0.14)
HPP	24.20 (0.64)*	23.54 (0.61)*	19.25 (0.44)	16.83 (0.39)	13.64 (0.76)*	13.86 (0.61)*	9.46 (0.42)	7.92 (0.31)
ANP	162.49 (0.33)	513.12 (0.66)*	645.68 (0.63)*	564.49 (0.50)	156.07 (0.30)	324.98 (0.31)	318.56 (0.31)	269.39 (0.4)
HNP	10.12 (0.46)	7.77 (1.03)*	16.04 (0.20)	13.57 (0.10)	6.79 (0.43)	7.09 (0.50)	2.65 (0.67)*	3.39 (0.60)*
MZP	121.41 (0.29)	211.1 (0.38)	340.17 (0.25)	286.57 (0.27)	179.38 (0.11)	216.57 (0.28)	130.16 (0.42)	52.5 (0.50)
MSP	4.90 (1.12)*	2.12 (1.18)*	8.02 (0.96)*	11.73 (1.25)*	0.48 (0.49)	0.34 (0.36)	0.24 (0.96)*	0.33 (1.07)*

Table 1 – Seasonal and spatial distribution of environmental and biological parameters. Abbreviations: DO- Dissolved oxygen, NO₃ - Nitrate, PO₄ - Phosphate, SiO₄ - Silicate, Chl. *a* - Chlorophyll *a*, APP -Autotrophic Picoplankton, HPP - Heterotrophic Picoplankton, ANP - Autotrophic Nanoplankton, HNP - Heterotrophic Nanoplankton, MZP - Microzooplankton and MSP-Mesozooplankton. Mean and coefficient of variations (in parentheses) are presented. * indicates significant tidal variation (P < 0.05). Locations 1 - 4 are represented as L1 - L4

Microzooplankton	Spring Intermonsoon (SIM)				Southwest Monsoon (SWM)			
	L1	L2	L3	L4	L1	L2	L3	L4
Ciliates								
<i>Codonellopsis</i>								
<i>orthoceros</i>	*	*	*	-	-	-	*	-
<i>C. schabi</i>	-	*	*	-	-	-	*	*
<i>Dictyocysta seshaiyai</i>	-	-	-	-	-	-	-	-
<i>Didinium nasutum</i>	0.22	0.08	*	0.11	0.02	0.12	*	-
<i>Euplotes moebiusi</i>	*	*	-	-	-	*	-	*
<i>Halteria chlorelligera</i>	-	*	-	-	-	-	*	*
<i>H. gradinella</i>	-	*	-	-	-	-	-	0.05
<i>Laboea strobila</i>	0.12	0.09	0.05	0.23	-	*	*	-
<i>Lohmaniella oviformis</i>	-	0.03	-	-	*	*	*	*
<i>L. spiralis</i>	0.02	0.16	0.02	0.03	*	*	0.04	0.06
<i>Stenosemella</i>								
<i>parvicollis</i>	-	0.03	*	-	-	-	0.03	*
<i>Strobilidium minimum</i>	*	0.03	-	*	*	*	*	-
<i>Strombidium bilobum</i>	*	*	*	*	0.03	-	*	*
<i>S. capitatum</i>	-	*	-	-	*	-	-	-
<i>S. conicum</i>	-	0.03	0.06	0.14	*	-	0.03	-
<i>S. sphericum</i>	-	-	-	-	-	-	*	0.06
<i>Tintinnidium incertum</i>	0.17	0.13	0.3	0.25	*	*	0.03	-
<i>T. primitivum</i>	0.15	0.11	0.27	0.14	0.1	0.05	0.03	-
<i>Tintinnopsis beroidea</i>	0.05	0.07	0.04	*	0.04	0.06	0.09	*
<i>T. cylindrica</i>	*	0.04	0.03	-	0.06	0.05	0.03	-
<i>T. lohmanni</i>	*	*	*	-	-	-	*	*
<i>T. minuta</i>	-	*	-	-	-	-	-	*
<i>T. nucula</i>	-	-	-	-	0.18	0.26	*	*
<i>T. radix</i>	-	*	-	-	-	-	-	-
<i>T. tocantinensis</i>	-	*	-	-	-	-	-	-
<i>T. uruguayensis</i>	*	0.03	0.05	-	-	-	*	*
H.Dinoflagellates								
<i>Gyrodinium spirale</i>	0.02	0.03	0.04	-	*	0.07	-	-
<i>Noctiluca scintillans</i>	-	*	*	*	-	-	-	*
<i>Protoperdinium</i>								
<i>depressum</i>	-	*	*	-	-	-	0.03	*
<i>P. globulus</i>	-	*	-	-	-	-	-	*
<i>P. leonis</i>	-	*	-	-	-	-	-	-

Table 2 - Microzooplankton composition and the species dominance during different seasons. Symbol * represents the species with low dominance values (<0.02). Minus sign implies absence of the species. Locations 1 - 4 are represented as L1 - L4

	Spatial variation between locations					
	L1 & L2	L1 & L3	L1 & L4	L2 & L3	L2 & L4	L3 & L4
SIM						
Salinity	-	**	**	*	**	-
DO	*	*	*	-	-	-
NO₃	*	*	*	*	*	*
PO₄	-	-	*	-	*	*
SiO₄	-	*	**	*	*	-
Chl. <i>a</i>	*	*	*	-	-	-
APP	-	*	**	**	**	-
HPP	-	*	*	**	**	-
ANP	-	*	*	*	*	-
HNP	-	*	*	*	*	-
MZP	-	**	**	*	*	-
MSP	-	*	*	*	*	-
SWM						
Salinity	-	*	**	*	**	-
DO	**	**	**	-	-	-
NO₃	*	*	*	*	*	*
PO₄	-	-	**	*	*	-
SiO₄	*	*	*	-	-	-
Chl. <i>a</i>	*	*	*	-	-	-
APP	-	*	*	**	**	-
HPP	-	*	*	*	-	-
ANP	*	*	*	-	-	-
HNP	-	**	**	**	**	-
MZP	-	*	**	*	**	-
MSP	-	*	*	-	-	-

Supplementary ANOVA Table 1 - Comparison of physicochemical and biological parameters based on non-parametric ANOVA. Symbols * and ** sequentially represents significance at 5% (P<0.05) and 0.1% level (p<0.001). Minus sign represents lack of significance. Abbreviations: SIM – Spring Intermonsoon, SWM- Southwest Monsoon, DO – Dissolved Oxygen, NO₂ - Nitrite, NO₃ – Nitrate, PO₄ - Phosphate, SiO₄ – Silicate, Chl. *a* – Chlorophyll *a*, APP - Autotrophic picoplankton, HPP – Heterotrophic Picoplankton, ANP - Autotrophic Nanoplankton, HNP – Heterotrophic Nanoplankton, MZP – Microzooplankton and MSP – Mesozooplankton. Locations 1 - 4 are represented as L1 - L4

Parameters	L1	L2	L3	L4
Salinity	**	**	**	**
Nitrate	*	NS	**	NS
Phosphate	NS	NS	NS	NS
Silicate	*	**	**	**
DO	NS	NS	NS	NS
Chl. <i>a</i>	**	NS	**	NS
APP	NS	NS	**	**
HPP	**	**	**	**
ANP	NS	NS	*	**
HNP	NS	NS	**	**
MZP	NS	NS	**	**
MSP	NS	NS	**	**

Supplementary ANOVA Table 2 – Variations in physico-chemical parameters between the Spring Intermonsoon and Southwest Monsoon seasons (* P<0.05; ** P<0.001). Locations 1 - 4 are represented as L1 - L4